Response of osteoblasts and preosteoblasts to calcium deficient and Si substituted hydroxyapatites treated at different temperatures

María Concepción Matesanz[a], Javier Linares[a], Mercedes Oñaderra[a], María José Feito[a], Francisco Javier Martínez-Vázquez[b,c], Sandra Sánchez-Salcedo[b,c], Daniel Arcos[b,c,*], María Teresa Portolés[a,*], María Vallet-Regí[b,c,*]

[a] *Department of Biochemistry and Molecular Biology I, Faculty of Chemistry, Universidad Complutense, 28040-Madrid, Spain*

[b] *Department of Inorganic and Bioinorganic Chemistry, Faculty of Pharmacy, Universidad Complutense, 28040-Madrid, Spain. Instituto de Investigación Sanitaria Hospital 12 de Octubre i+12, 28040-Madrid, Spain*

[c] *CIBER de Bioingeniería, Biomateriales y Nanomedicina (CIBER-BBN)*

* Corresponding authors. *E-mail address:* arcosd@ucm.es, portoles@quim.ucm.es, vallet@ucm.es.

ABSTRACT

Hydroxyapatite (HA) is a calcium phosphate bioceramic widely used for bone grafting and augmentation purposes**.** The biological response of HA can be improved through chemical and microstructural modifications, as well as by manufacturing it as macroporous implants. In the present study, calcium deficient hydroxyapatite (CDHA) and Si substituted hydroxyapatite (SiHA) macroporous scaffolds have been prepared by robocasting. In order to obtain different microstructural properties, the scaffolds have been treated at 700ºC and 1250ºC. The scaffolds have been characterized and tested as supports for both osteoblast growth and pre-osteoblast differentiation, as fundamental requisite for their potential use in bone tissue engineering. Morphology, viability, adhesion, proliferation, cell cycle, apoptosis, intracellular content of reactive oxygen species and interleukin-6 production were evaluated after contact of osteoblasts-like cells with CDHA and SiHA materials. An adequate interaction of osteoblasts-like cells and preosteoblasts-like cells with all these scaffolds was observed. However, the higher bone cell proliferation and differentiation on CDHA and SiHA scaffolds treated at 1250ºC and the lower adsorption of albumin and fibrinogen on these materials in comparison to those treated at 700ºC, suggest a better tissue response to CDHA and SiHA materials treated at high temperature.

1. Introduction

Calcium phosphate (CaP) bioceramics, both of natural and synthetic origin, are among the biomaterials of choice to fabricate scaffolds for *in situ* bone regeneration and tissue engineering purposes [1-3]. These scaffolds are designed to act as temporary templates for migration, proliferation and differentiation of osteoblasts, which are the cells responsible for new bone formation [4-6]. Many tissue engineering strategies are based on combinations of scaffolds with cells and different growth factors [7-9]. These constructs are commonly designed to mimic the interconnected porosity of cancellous bone, to stimulate the differentiation of mesenchymal stem cells towards osteoblast phenotype and to promote angiogenesis. It is widely accepted that macroporous scaffolds should exhibit interconnected porous architectures, with pores ranging in size between 200 μm and 800 μm, to be considered as appropriated for cell colonization and angiogenesis [10,11]. In this sense, the use of rapid prototyping techniques allows for an accurate control of the scaffold architecture and allows the design of the scaffold morphology for each specific defect [12-14].

Among the different CaP based bioceramics, hydroxyapatite (HA) implants are the most widely used for bone grafting and augmentation purposes [15,16]. The good i*n vivo* behaviour of HA relies on the partial dissolution/precipitation events which take place in contact with biological fluids together with cell-mediated mechanisms [17,18]. Porosity and particle size affect the degradation rate of the compound and the biological response of the implant [19,20]. Synthetic HA is commonly prepared at temperatures above 1000ºC, which results in highly crystalline stoichiometric compounds. In order to enhance the bioreactivity of HA based bone

grafts, several modifications have been proposed such as the preparation of calcium deficient hydroxyapatite (CDHA) [21], low temperature methods [22] and silicon incorporation (Si-HA) [23-25] among other strategies. Apatite based bioceramics treated at temperatures below 900ºC result in materials with many microstructural defects (such as high microporosity and incomplete sintering), which show crystallites smaller than 50 nm in size [21,24]. Since these features facilitate the dissolution and reactivity with the environment, manufacturing 3D macroporous scaffolds with nanocrystalline ceramics is a very interesting strategy to enhance tissue regeneration in bone defects treated with these grafts. Unfortunately, the mechanical properties of these implants are very poor, involving a serious drawback for skeletal applications. Therefore their sintered derivatives must be also considered.

Cell adhesion onto the scaffold surface is essential for implant integration and subsequent tissue regeneration. Cell attachment is governed by the chemistry and surface topography of the scaffolds, as both factors determine the kind and amount of adsorbed proteins. It is well known that implanted materials are immediately coated with proteins from blood and interstitial fluids. Extracellular matrix glycoproteins, such as fibronectin and vitronectin, are key mediators of cell behaviour and play an important role in cell adhesion on scaffolds, cell migration and differentiation processes, required for tissue repair [28]. Thus, the scaffold physicochemical properties and the pattern in which adhesion proteins and other bioactive molecules adsorb to scaffold surface, determine the specific cell reactions after implantation. *In vitro* studies have demonstrated favourable cell responses to charged hydrophilic surfaces, due to the superior adsorption and bioactivity of adhesion proteins [28].

In the present study, calcium deficient hydroxyapatite (CDHA) and Si substituted hydroxyapatite (SiHA) macroporous scaffolds have been prepared by robocasting. In order to

obtain different microstructures, both types of scaffolds have been heated at 700ºC and 1250ºC. Afterwards, the resulting scaffolds have been tested as support for bone cell growth, as fundamental requisite for their potential use in bone tissue engineering. With this objective, human Saos-2 osteoblast-like cells were cultured in contact with CDHA and SiHA materials, evaluating different cell parameters as morphology, viability, adhesion, proliferation, cell cycle, apoptosis and intracellular content of reactive oxygen species (ROS). The adsorption of culture medium proteins and specific serum proteins (bovine serum albumin and fibrinogen) was also measured on the surface of these materials.

2. Materials and methods

2.1. Silicon substituted hydroxyapatite (SiHA) and calcium deficient hydroxyapatite (CDHA) synthesis

Silicon-substituted hydroxyapatite (Si-HA) with nominal formula $Ca_{10}(PO_4)_{5.7}(SiO_4)_{0.3}(OH)_{1.7}\square_{0.3}$ (where □ means vacancies at the hydroxyl position) and calcium deficient hydroxyapatite (CDHA) with nominal formula $Ca_{9.6}\square_{0.4}(PO_4)_{5.6}(HPO_4)_{0.4}(OH)_2$ (where □ means vacancies at the Ca position) were prepared by aqueous precipitation reaction of $Ca(NO_3)_2{\cdot}4H_2O$, $(NH_4)_2HPO_4$ and $Si(CH_3CH_2O)_4$ solutions. The concentrations were adjusted to have a Ca/P+Si ratio of 1.67 for Si-HA and Ca/P ratio of 1.6 for CDHA.

The solutions were slowly casted into the preheated reactor and stirred for 12 h at 80°C. The pH was kept at 9.5 by NH_3 solution addition. During the reaction the pH was continuously adjusted to 9.5 to ensure constant conditions during the synthesis. The precipitated powders were aged within their mother liquor for 24 hours, and dried at 100ºC for 24 hours. In order to remove residual nitrates and/or carbonates, the powders were treated at 700ºC for 1 hour. Finally, the

powders were milled in a planetary ball milling device (Pulverisette 6, Fritsch) and sieved to 75 μm.

2.2. Preparation of 3D scaffolds

SiHA and CDHA ceramic inks for robocasting with a final solid content of 30 vol.% were prepared as follows: first, a stable suspension was prepared by dissolving 2.5 wt.% (relative to powder content) Darvan® C dispersant (R.T. Vanderbilt, Norwalk, CT) in distilled water and gradually adding the ceramic powder. An appropriate amount (7 mg per mL of liquid in the final suspension) of previously dissolved hydroxypropyl methylcellulose (Methocel F4 M, Dow Chemical Co., Midland, MI) was then added to the mixture to increase the viscosity. Subsequently, the ink was gellified by adding 4 vol.% (relative to liquid content) polyethylenimine (PEI) as flocculant. After each addition the mixture was placed in a planetary centrifugal mixer (ARE-250, Thinky Corp., Tokyo, Japan) for a few minutes at 800-1200 r.p.m. to improve its homogeneity and stability. Three-dimensional scaffolds were constructed via direct-write assembly of the fabricated inks using a robotic deposition device (EnvisionTEC GmbH 3-D BioplotterTM). The printing syringe was partially filled with the ink, tapped vigorously under slight vacuum to remove bubbles, and then placed on the three-axis motion stage controlled independently by a computer aided direct-write program (PRIMCAM version 2.98). The inks were deposited through conical deposition nozzles (smooth-flow tapered tips, Nordson EFD) of a diameter of 500 μm at the volumetric flow rate required to maintain a constant x–y printing speed. Each layer in the computer 3-D model of the structure consisted of parallel rods with a center-to-center spacing s = 1200 μm. Rods in adjacent layers were orthogonal and the spacing between layers was set to h = 350 μm. The external dimensions of the scaffolds were set at about 14 mm of diameter and 20 deposited layers.

The samples were dried in air at room temperature for at least 24 h, and then heated in a furnace at 700 °C (1 °C/min heating rate) for 1 h to evaporate the organics, resulting in scaffolds SiHA-700 and CDHA-700. The sintered scaffolds were heated at 1250 °C (3 °C/min heating rate) for 1 h to avoid microcracking in the sintered body associated to the residual stress generated during the β↔α phase transition due to the differences in density between β-TCP (3.07 $g \cdot cm^{-3}$) and α-TCP (2.86 $g \cdot cm^{-3}$). The thermal treatment at 1250ºC was chosen after measuring the scaffolds strut density and compressive strength for a range of temperatures between 1100ºC and 1300ºC (Figure S1 in supporting info). These scaffolds are labeled as SiHA-1250 and CDHA-1250.

2.3. Characterization: chemical, structural and microstructural studies of CDHA and SIHA

Elemental chemical analysis was carried out by fluorescence X-ray spectrometry for P, Si and Ca. X-ray diffraction (XRD) patterns were collected with a Philips PW 1730 X-ray diffractometer using Cu Kα radiation with a step size of 0.02 2θº and 8 seconds of counting time. In order to determine the crystalline and microstructural features of both samples, Rietveld refinements were carried out over the XRD patterns collected. The refinements were performed using the atomic position set and the space group of the HA structure $P6_3/m$, no 176 by means of FullProf 2000 software.

The textural properties of the calcined materials were determined by nitrogen adsorption/desorption analyses at -196ºC on a Micromeritics ASAP 2020 instrument (Micromeritics Co, Norcross, USA). To perform the N_2 adsorption measurements, 100-150 mg of materials were previously degassed under vacuum for 24 h, at 200°C. The surface area was determined using the Brunauer-Emmett-Teller (BET) method. The pore size distribution between

0.5 and 40 nm was determined from the adsorption branch of the isotherm by means of the Barret-Joyner-Halenda (BJH) method.

Scanning electron microscopy was carried out with a JEOL 6400 Microscope-Oxford Pentafet super ATW microscope and elemental chemical analyses were carried out by fluorescence X-ray spectrometry for P, Si and Ca. Fourier transform infrared (FTIR) spectroscopy were carried out on powdered materials with a Nicolet Magma IR 550 spectrometer.

2.4. Adsorption of bovine serum albumin (BSA) on powdered CDHA and SiHA

Adsorption experiments were carried out with 10 mg of powdered samples incubated with a solution of BSA (Sigma A2058) at 1.35 $mg \cdot mL^{-1}$ in PBS and moderately shaken for 4 h at 37ºC. No significant difference was detected between the amount of adsorbed protein after 4 h and 24 h. Controls with the same BSA concentration but without material were carried out. After incubation time, the supernatant obtained was analyzed by UV-Vis spectroscopy and the adsorbed protein amount was calculated as the difference in protein concentration before and after BSA adsorption using a value of 0.667 as extinction coefficient *E* (279 nm, 1cm and 0.1% solution of BSA).

2.5. Adsorption of bovine fibrinogen on powdered CDHA and SiHA

Analysis of the fibrinogen (Sigma F8630) adsorption was performed by incubation at 37ºC for 4h of 10 mg of either CDHA or SiHA with a solution of this protein (1 $mg \cdot mL^{-1}$) in PBS. The amount of protein which did not sediment after centrifugation was determined from the absorbance spectra of the supernatants, and the percentage of adsorbed fibrinogen was then calculated considering the initial concentration of protein as reference.

2.6. Adsorption of culture medium proteins on 3D scaffolds of CDHA and SiHA

The total content of culture medium proteins adsorbed on 3D scaffolds of CDHA and SiHA was determined by a colorimetric method at 540 nm (Bio-Analítica, S.L.), using a Beckman DU 640 UV-Visible spectrophotometer.

2.7. Culture of osteoblast-like cells with powdered CDHA and SiHA

Human Saos-2 osteoblasts-like cells (10^5 cells/mL) were cultured in the presence of 1mg/mL of each material in Dulbecco´s Modified Eagle´s Medium (DMEM, Sigma Chemical Company, St. Louis, MO, USA) supplemented with 10% (vol/vol) fetal bovine serum (FBS, Gibco, BRL), 1 mM L-glutamine (BioWhittaker Europe, Belgium), penicillin (200 µg/mL, BioWhittaker Europe, Belgium), and streptomycin (200 µg/mL, BioWhittaker Europe, Belgium), under a 5% CO_2 atmosphere and at 37ºC for 48 hours. Tissue culture plastic (TCP) was used as control surface in the absence of materials. To evaluate the cell proliferation on the substrates, the medium was aspirated and the attached cells were harvested using 0.25% trypsin-EDTA solution and counted with a Neubauer hemocytometer. The non-attached cells were previously discarded by washing the cultures with PBS.

2.8. Culture of osteoblast-like cells on 3D scaffolds of CDHA and SiHA

Saos-2 osteoblast-like cells ($3x10^5$ cells/mL) were seeded directly onto scaffolds in 24-well plates and were cultured for 48 h, in Dulbecco´s Modified Eagle´s Medium (DMEM, Sigma Chemical Company, St. Louis, MO, USA) supplemented with 10% (vol/vol) fetal bovine serum (FBS, Gibco, BRL), 1 mM L-glutamine (BioWhittaker Europe, Belgium), penicillin (200 µg/mL,

BioWhittaker Europe, Belgium), and streptomycin (200 µg/mL, BioWhittaker Europe, Belgium), under a 5% CO_2 atmosphere and at 37ºC.

2.9. Flow Cytometry studies

After incubation with the different probes, as is described below, the conditions for the data acquisition and analysis were established using negative and positive controls with the CellQuest Program of Becton Dickinson. These conditions were maintained during all the experiments. At least 10,000 cells were analysed in each sample.

2.9.1. Cell cycle analysis and apoptosis detection

Cell suspensions were incubated with Hoechst 33258 (PolySciences, Inc., Warrington, PA) (Hoechst 5µg/mL, ethanol 30%, and BSA 1% in PBS), used as a nucleic acid stain, during 30 min at room temperature in darkness. The fluorescence of Hoechst was excited at 350 nm and the emitted fluorescence was measured at 450 nm in a LSR Becton Dickinson Flow Cytometer. The cell percentage in each cycle phase: G0/G1, S and G2/M was calculated with the CellQuest Program of Becton Dickinson and the SubG1 fraction was used as indicative of apoptosis.

2.9.2. Intracellular reactive oxygen species (ROS) content and cell viability

Cells were incubated at 37ºC for 30 min with 100 µM 2´,7´-dichlorofluorescein diacetate (DCFH/DA, Serva, Heidelberg/ Germany) for directly measuring the intracellular content of ROS. DCFH/DA is diffused into cells and is deacetylated by cellular esterases to non-fluorescent DCFH, which is rapidly oxidized to highly fluorescent DCF by ROS. To measure the intracellular reactive oxygen species (ROS), the DCF fluorescence was excited by a 15 mW laser tuning to 488 nm and the emitted fluorescence was measured with a 530/30 band pass filter in a FACScalibur Becton Dickinson Flow Cytometer. Cell viability was determined by propidium

iodide (PI) exclusion test and flow cytometry after addition of PI (0.005% in PBS, Sigma-Aldrich Corporation, St. Louis, MO, USA) to stain the DNA of dead cells.

2.10. Morphological Studies by Scanning Electron Microscopy

Scanning electron microscopy was carried out with a JEOL JSM-6400 scanning electron microscope. Cells cultured on 3D scaffolds of either CDHA or SiHA were fixed with glutaraldehyde (2.5% in PBS) for 45 min. Sample dehydration was performed by slow water replacement using series of ethanol solutions (30, 50, 70, 90%) for 15 min with a final dehydration in absolute ethanol for 30 min, allowing samples to dry at room temperature and under vacuum. Afterwards, the pieces were mounted on stubs and coated in vacuum with gold-palladium.

2.11. Differentiation studies with preosteoblast-like cells.

Murine MC3T3-E1 preosteoblast-like cells (as undifferentiated osteoblast-like cells) were seeded at a density of 5 x 10^4 cells/mL directly onto scaffolds in 24-well plates in DMEM with 10% fetal bovine serum (FBS, Gibco, BRL), 1 mM L-glutamine (BioWhittaker Europe, Belgium), penicillin (200 µg/mL, BioWhittaker Europe, Belgium), streptomycin (200 µg/mL, BioWhittaker Europe, Belgium), β-glycerolphosphate (50 µg/mL, Sigma Chemical Company, St. Louis, MO, USA) and L- ascorbic acid (10 mM, Sigma Chemical Company, St. Louis, MO, USA), under a CO_2 (5%) atmosphere at 37ºC for 7 days. Alkaline phosphatase (ALP) activity was used as the key differentiation marker in assessing expression of the osteoblast phenotype. ALP activity and the protein total value were determined by commercial kits Spinreact (Bio Analitica S.L.).

2.12. Mitochondrial activity

MTT method was employed to evaluate the mitochondrial redox activity of either Saos-2 osteoblast-like cells or MC3T3-E1 preosteoblast-like cells cultured on 3D scaffolds after 48 h and 7 days, respectively. This test is based in the reduction of yellow 3[4,5-dimethylthiazol-2yl]-2,5-diphenyltetrazolium bromide to blue formazan [29]. For this, the culture media were replaced with 1 mL of DMEM and 125 µL of 0.012 g/L MTT solution in PBS. Samples were incubated for 4 h at 37ºC and 5% CO_2 in dark conditions. Then, the medium was removed and 500 µL of isopropanol:HCl 0.4 N were added. Finally, the absorbance was measured at 570 nm using a Beckman DU 640 UV-Visible spectrophotometer. Controls without cells were carried out in order to subtract the colorant retained by the material.

2.13. Interleukin 6 (IL-6) detection

The amount of IL-6 in the culture medium was quantified by ELISA (Gen-Probe, Diaclone), carried out according to the manufacturer's instructions.

2.14. Statistics

Data are expressed as means ± standard deviations (SD). All the experiments were performed twice and carried out in triplicate (n=6). Statistical analysis was performed using the Statistical Package for the Social Sciences (SPSS) version 19 software. Statistical comparisons were made by analysis of variance (ANOVA). Scheffé test was used for *post hoc* evaluations of differences among groups. In all of the statistical evaluations, $p < 0.05$ was considered as statistically significant.

3. Results and discussion

3.1. Characterization of calcium deficient hydroxyapatite (CDHA) and Si substituted hydroxyapatite (SiHA) 3D scaffolds

Fig. 1a shows the XRD patterns corresponding to scaffolds SiHA-700 and CDHA-700. Both patterns show a single apatite-like phase with broadened diffraction maxima. The microstructural study (derived from the Rietveld analysis) indicates that the crystallite sizes are 23.5 and 33.4 nm for CDHA-700 and SiHA-700, respectively (see Table 1). Figure 1.b shows the XRD patterns corresponding to scaffolds CDHA-1250 and SiHA-1250. The thermal treatment at 1250ºC lead to the enlargement of the crystallite size up to 77.5 nm and 63.6 nm for CDHA-1250 and SiHA-1250, respectively (Table 1). XRD patterns evidence that CDHA-1250 and SiHA-1250 are not single crystalline phases but biphasic calcium phosphates (BCP) that result from the segregation of a secondary α–TCP phase after the thermal treatment at 1250ºC. The formation of a biphasic calcium phosphate (BCP) of hydroxyapatite and α–TCP was expected for sample CDHA-1250. In fact, the thermal decomposition of calcium deficient HA is one of the methods to obtain BCPs. The segregation of α–TCP during the thermal treatment of SiHA could be explained in terms of the stabilization of this phase when HA is heated in presence of silicon, as it has been previously reported elsewhere [30]. The phase composition and the crystallite size parameters are shown in Table 1. Therefore, CDHA-1250 scaffolds are not calcium deficient hydroxyapatites, but HA/α-TCP biphasic calcium phosphates formed after treating CDHA at 1250ºC. Similarly, SiHA-1250 is not a single silicon substituted hydroxyapatite phase, but a SiHA/α-TCP biphasic calcium phosphate formed after treating SiHA at 1250ºC. The labels CDHA-1250 and SiHA-1250 are kept for clarity purposes and indicate that these samples come from the thermal treatment at 1250º C of CDHA and SiHA precursors, respectively.

Fig. 2 shows the SEM images of the different scaffolds. The structures shown in Figs. 2a and 2c correspond to the top and lateral view of SiHA-700, respectively. The scaffolds exhibit high uniformity with struts of 475 μm diameter and macropores of 520 μm in size from a top view, macropores of 190 μm in size from the lateral view. While the larger channels (520 μm) are distributed in the porous lattice to offer space for blood vessel to grow deep into the scaffold, the smaller pores (190 μm) array is aimed to provide strength, and higher surface area to support new bone formation. Despite the structure shrinkages due to the sintering process, SiHA-1250 scaffolds keep the high uniformity. This is clearly evidenced when comparing the microstructural characteristic of SiHA-700 (Fig. 2e) and SiHA-1250 (Fig. 2f). While SiHA-700 exhibits a porous surface formed by agglomerates made of small nanoparticles, SiHA-1250 shows a dense surface where particles appear sintered as a consequence of the thermal treatment.

Table 1 also shows the textural parameters and the surface charge of the scaffolds. The surface area values for CDHA-700 and SIHA-700 are 20 and 37 $m^2 \cdot g^{-1}$, respectively. These values are significantly reduced when the scaffolds are treated at 1250ºC, showing values of 1.1 $m^2 \cdot g^{-1}$ or less, as a consequence of the densification process. CDHA-700 and SIHA-700 contain pores of 11.5 nm in size. These mesopores are in the order of magnitude of crystallite size as determined by XRD and indicate that the crystallites of low temperature scaffolds remain separated, leaving mesopores between them. After the thermal treatment at 1250ºC, the crystallites grow and the porosity at the nanometer scale disappears. Table 1 also indicates that the surface charge of all the scaffolds remain negative independently of the silicon content and the thermal treatment, as would correspond for calcium hydroxyapatites. Mechanical properties were also enhanced with

the thermal treatment. The scaffolds treated at 1250ºC showed the maximum strut density values of 90% and compressive strength values of 50 MPa (see supporting info).

3.2. Effects of powdered calcium deficient hydroxyapatite (CDHA) and Si substituted hydroxyapatite (SiHA) on human Saos-2 osteoblast-like cells

In order to evaluate the bone cell response to CDHA and SiHA materials treated at 700ºC and 1250ºC, before carrying out the studies with 3D scaffolds, human Saos-2 osteoblasts were cultured in contact with these four materials in powdered form evaluating different cell parameters. The powders properties were analysed by XRD diffraction, Fourier Transform Infrared (FTIR) spectroscopy and zeta potential measurements. XRD patterns showed the same phase composition and microstructural characteristics as those obtained from the corresponding scaffolds. FTIR spectra (Figure S2 in supporting info) showed the absorption bands corresponding to phosphates and hydroxyl groups in both 700ºC and 1250ºC treated powders. None of them showed bands corresponding to carbonates, nitrates or any other residuals that could affect the cell viability. Zeta potential measurements were almost identical than those shown in Table 1.

Saos-2 osteoblast-like cell proliferation and viability were evaluated after 48 hours in contact with 1 $mg \cdot mL^{-1}$ of powdered materials. The cells spread and grew showing viability values of 90 % (Figure S3). However, the cell proliferation significantly decreased as it has been previously observed for calcium phosphate ceramics treated at low temperature [31]. Non-significant differences in cell number were observed among the four powdered materials after 48 hours of treatment.

Proliferation is dependent on the cell cycle progression, in which cells pass through the G0/G1 phase (Quiescence/Gap 1) to the S phase (Synthesis) and finally to the G2/M phase (Gap 2 and Mitosis). To evaluate if the cell proliferation delay observed in the presence of these powdered materials is accompanied by some cell cycle alterations, the analysis of cell cycle phases of Saos-2 osteoblast-like cells cultured in the presence of 1 $mg \cdot mL^{-1}$ of powdered samples was carried out after 48 hours of treatment. The SubG1 fraction, corresponding to cells with fragmented DNA, was used as indicative of apoptosis. No significant alterations were observed in G0/G1, S and G2/M phases after treatment with these four materials and the analysis of SubG1 fraction reveals low apoptosis levels in all cases (Fig. 3). However, a slight but significant apoptosis increase was induced by CDHA-700, SiHA-700 and SiHA-1250. Since apoptosis is generally associated with the increase of intracellular reactive oxygen species (ROS) [32-34], the effects of 1 $mg \cdot mL^{-1}$ of the four powdered samples on intracellular ROS content of Saos-2 were studied after 48 hours (Figure S4). The materials did not increase intracellular ROS content of Saos-2 cells and non-significant ROS differences were observed between CDHA and SiHA at the same temperature. The absence of oxidative stress suggests that the low apoptosis levels observed in Fig. 3 (Sub G1 fraction) are due to weak contacts between the cell and the support (tissue culture plastic) in the presence of these powdered materials which can trigger a kind of apoptosis defined as anoikis, induced by loss of cell anchorage [35].

Interleukin IL-6 plays a protective role by enhancing the intracellular antioxidant reserve of glutathione in different cell types [36,37]. For this reason the levels of this cytokine were measured in the medium of osteoblasts cultured 48 hours in contact with 1 $mg \cdot mL^{-1}$ of powdered samples (Figure S4). The treatment with 1 $mg \cdot mL^{-1}$ of powdered CDHA-1250 produced a

significant decrease of IL-6, whereas SiHA-1250 elicits an increase of IL-6 respect to the control (TCP). These results suggest a beneficial effect of the silicon presence in powdered SiHA-1250.

3.3. Adhesion and proliferation of human Saos-2 osteoblasts-like cells on 3D robocasted scaffolds

Macroporous 3D scaffolds are aimed to create an adequate microenvironment for bone cell growth by means of mimicking the porous architecture of natural bone [5,38]. In the present study, a rapid prototyping technique such as 3D robocasting was used to prepare ceramic scaffolds with the synthesised materials. Saos-2 osteoblasts-like cells were cultured for 48 hours on these supports, evaluating their capability to keep cellular adhesion and proliferation on their surfaces.

Fig. 4 shows the SEM micrographs obtained of Saos-2 cells cultured during 48 hours onto the scaffolds surface. SEM images evidence the attachment of Saos-2 onto the surfaces. The cells show the typical morphology of osteoblast like cells, *i.e.* cube-shaped, big sized and exhibit long cytoplasmic prolongations to adhere to the surface. These results indicate a good biocompatibility and an adequate interaction of osteoblasts with the scaffolds prepared, independently of their chemical composition and microstructure.

Cell viability and proliferation of Saos-2 osteoblasts-like cells were indirectly evaluated by measuring mitochondrial redox activity by MTT test after 48 hours of culture (Figure 5). The mitochondrial activity indicates that osteoblast proliferation on CDHA-1250 and SiHA-1250 scaffolds was significantly higher ($p<0.005$) than on CDHA-700 and SiHA-700 scaffolds.

3.4. Adsorption of culture medium proteins on 3D macroporous scaffolds

Cells attach and spread when in contact with an adequate surface through adhesion proteins-dependent processes. The quality of cell attachment affects the cell morphology as well as their proliferation and differentiation capability [28]. Therefore, the interaction of osteoblasts with bone matrix is an essential event for their differentiation and it is required to develop the specific activities of these cells [39]. Integrins are the major cell receptors involved in the cell-binding-to-matrix proteins, such as fibronectin, type I collagen and vitronectin, via the RGD-sequences [39]. Under *in vitro* conditions, the adsorption of these proteins from culture medium determines the early non-specific stage of cell adhesion, facilitating cell spreading on the scaffolds through the formation of a conditioning protein layer that promotes cell adhesion, differentiation and extracellular matrix production [40,41].

Figure 5 also shows the amount of adsorbed protein onto the scaffolds surfaces. CDHA-1250 and SiHA-1250 adsorb lower amounts of proteins compared with the scaffolds treated at 700ºC. However, Saos-2 osteoblast-like cells rather proliferate onto CDHA-1250 and SiHA-1250 than onto CDHA-700 and SiHA-700, as it is evidenced by the mitochondrial activity also shown in Figure 5 (up). The higher amount of proteins adsorbed onto CDHA-700 and SiHA-700 scaffolds can be explained on the basis of their textural properties. The surface area and porosity of the struts is significantly higher in CDHA-700 and SiHA-700 compared with CDHA-1250 and SiHA-1250, as it can be seen in Table 1. The surface area and porosity facilitate the wettability of the scaffolds and provide much more contact points for protein anchorage. Table 1 also shows that CDHA-700 and SiHA-700 scaffolds exhibit strut porosity in the mesopore range and the average crystallite size is below 35 nm, pointing out that they are nanocrystalline materials. On the contrary, the highly sintered CDHA-1250 and SiHA-1250 scaffolds, with very low surface areas and porosities, are not able to adsorb the large amount of proteins found in CDHA-700 and

SiHA-700. Moreover, the crystallite sizes of CDHA-1250 and SiHA-1250 are much larger, thus leading to lower surface energy and less protein adsorption. Since the proteins interact at the nanometric level with the surfaces and the surface energy is higher in nanostructured materials, the high protein adsorption in CDHA-700 and SiHA-700 is justified by both textural and thermodynamic reasons.

In principle, higher amounts of proteins adsorbed onto the scaffold surface should increase the cell adhesion and proliferation. However osteoblast-like cells proliferate better on CDHA-1250 and SiHA-1250 scaffolds. This fact can be attributed to the low sintered surfaces and nanocrystalline nature of CDHA-700 and SiHA-700. The nanoparticles detachment and loosening of anchoring elements in CDHA-700 and SiHA-700 seem to result in some degree of anoikis, in a similar way than that observed when osteoblasts are seeded in the presence of powdered samples.

3.5. Adsorption of serum albumin (BSA) and fibrinogen on powdered calcium deficient hydroxyapatite (CDHA) and Si substituted hydroxyapatite (SiHA)

Blood and interstitial fluid proteins adsorb onto the biomaterial surface immediately after taking contact. This protein adsorption process determines the future success or failure of the implant [42,43]. The adhesion of albumin, fibrinogen and other serum proteins to biomaterials has been related with negative effects such as infections and thrombogenicity, mainly due to the enhancement of bacteria-surface interactions and platelet adhesion [44-46]. In the present study, the adsorption of specific serum proteins as bovine serum albumin (BSA) and fibrinogen was measured on powdered CDHA and SiHA treated at 700ºC and 1250ºC.

As it can be observed in Fig. 6, the amount of BSA and fibrinogen adsorbed on powdered samples treated at 1250ºC was significantly lower than on these materials treated at 700ºC ($p<0.005$), in agreement with the culture medium protein adhesion observed on 3D scaffolds of these hydroxyapatites (Fig. 5, Proteins). The adsorption of both BSA and fibrinogen on powdered SiHA treated at 700ºC was significantly lower than on powdered CDHA treated at the same temperature. However, the absorption of this two serum proteins on powdered SiHA-1250 was significantly higher than on powdered CDHA-1250.

It is widely accepted that the amount of adsorbed fibrinogen and, more specifically, its conformation are important factors for platelet adhesion which determines the hemocompatibility of a given biomaterial [47]. On the other hand, recent studies demonstrate a reduced in vitro bioactivity of HA surface coated with BSA in comparison to the uncoated surface [48]. The lower BSA and fibrinogen adsorption on samples treated at 1250ºC compared with those treated at 700ºC suggests a better tissue response to CDHA-1250 and SiHA-1250 scaffolds, in agreement with the cell proliferation results (Fig. 5, Mitochondrial activity).

3.6. Proliferation and differentiation of MC3T3 preosteoblast-like cells on calcium deficient hydroxyapatite (CDHA) and Si substituted hydroxyapatite (SiHA) 3D scaffolds

In order to know the effects of the scaffolds on the differentiation of bone cells, undifferentiated MC3T3 preosteoblast-like cells were seeded on the different 3D scaffolds. The cell proliferation and alkaline phosphatase activity (as the key differentiation marker in assessing expression of the osteoblast phenotype) were evaluated. Fig. 7 (up) shows that preosteoblast-like cells proliferation was significantly higher on CDHA-1250 and SiHA-1250 scaffolds than on CDHA-700 and SiHA-700 scaffolds, in agreement with the results obtained with Saos-2 (Fig. 5,

Mitochondrial activity). Concerning cell differentiation, the ALP results obtained with these scaffolds (Fig. 7, ALP) indicate a higher bone cell differentiation on CDHA-1250 and SiHA-1250 than on CDHA-700 and SiHA-700 scaffolds, especially on SiHA-1250, which would suggest a better tissue response at implantation sites of SiHA-1250 scaffolds, enhancing bone formation.

4. Conclusion

3D scaffolds of calcium deficient hydroxyapatite (CDHA) and Si substituted hydroxyapatite (SiHA) treated at either 700ºC or 1250ºC were evaluated as supports for bone cell growth as a fundamental requisite for their potential use in bone tissue engineering. The scaffolds treated at 700ºC resulted in nanocrystalline CDHA and SiHA materials with higher surface areas and porosities. Besides, the heating at 1250ºC of CDHA and SiHA resulted in highly crystalline biphasic α-TCP/HA materials. An adequate interaction of osteoblast-like cells and preosteoblast-like cells was observed with all the scaffolds. However, scaffolds treated at 1250ºC exhibit higher cell proliferation and differentiation, lower adsorption of albumin and fibrinogen and better mechanical properties in comparison to those treated at 700ºC. The poor cell response observed in contact with CDHA and SiHA materials treated at low temperature could be due to the surface topography of these materials which could induce a loss of cell anchorage over poorly sintered surfaces. These results suggest a better tissue response to CDHA and SiHA materials treated at high temperature, enhancing bone formation after *in vivo* implantation.

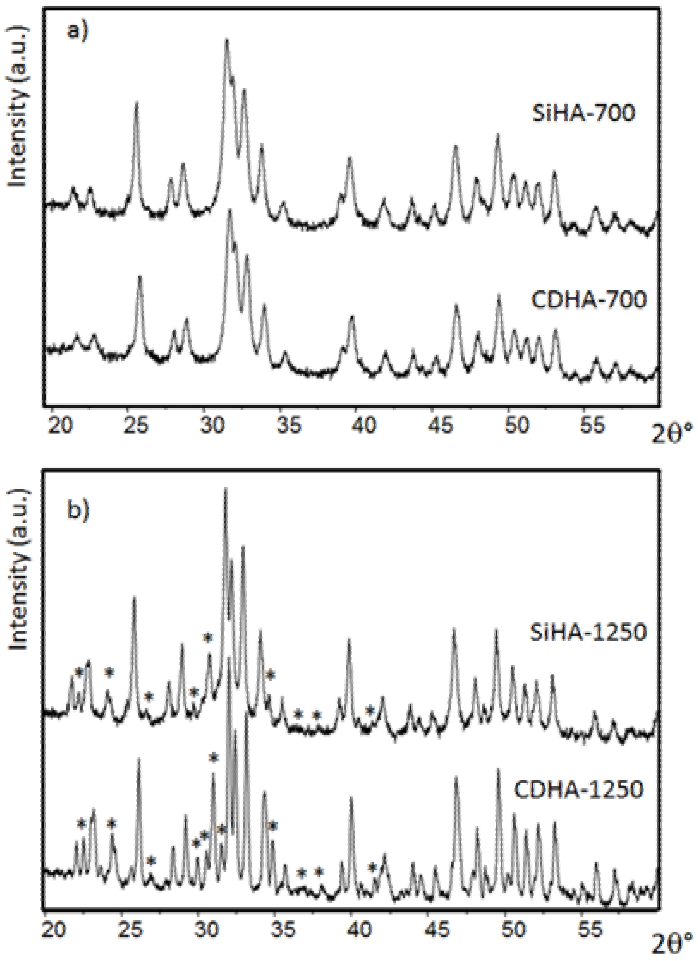

Figure 1. XRD patterns corresponding to (a) samples treated at 700ºC and (b) 1250ºC. The *symbols mark the position of the peaks of α–TCP phase.

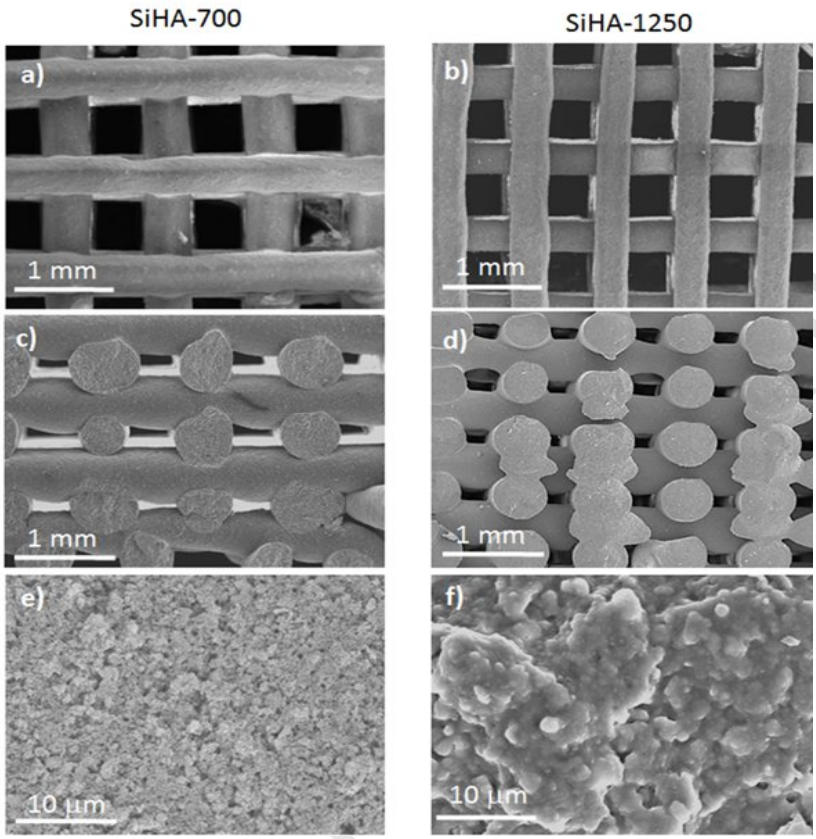

Figure 2. SEM micrographs for the Si-HA scaffolds treated at 700ºC obtained from (a) top view, (c) lateral view (c) fracture surface. Scaffolds treated at 1250ºC are also shown in (b) top view, (d) lateral view (f) fracture surface. The scaffolds made of CDHA showed almost identical characteristics for similar thermal treatments.

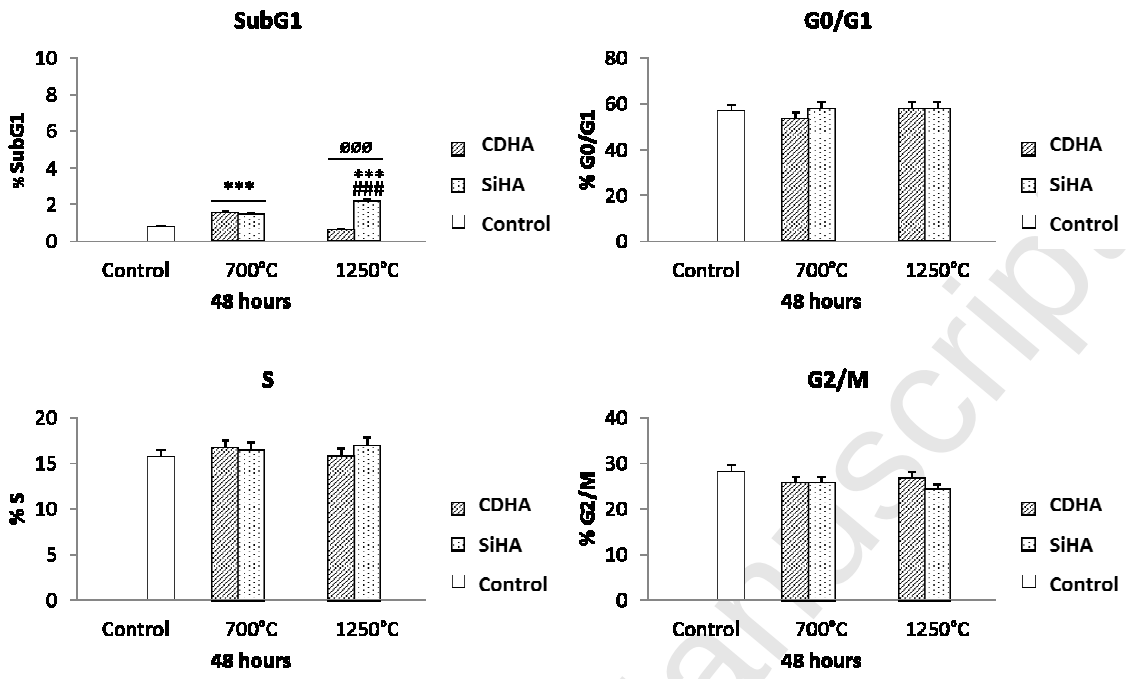

Figure3. Effects of 1 mg·mL^{-1} of powdered CDHA and SiHA treated at either 700ºC or 1250ºC on cell cycle phases of Saos-2 osteoblast-like cells after 48 hours treatment. Data are expressed as means ± standard deviations (SD). All the experiments were performed twice and carried out in triplicate (n=6). Statistical significance: ***$p<0.005$ (compared to control without material), # (comparison between CDHA and SiHA at the same temperature), ϕ (comparison between the same material at 700ºC and 1250ºC).

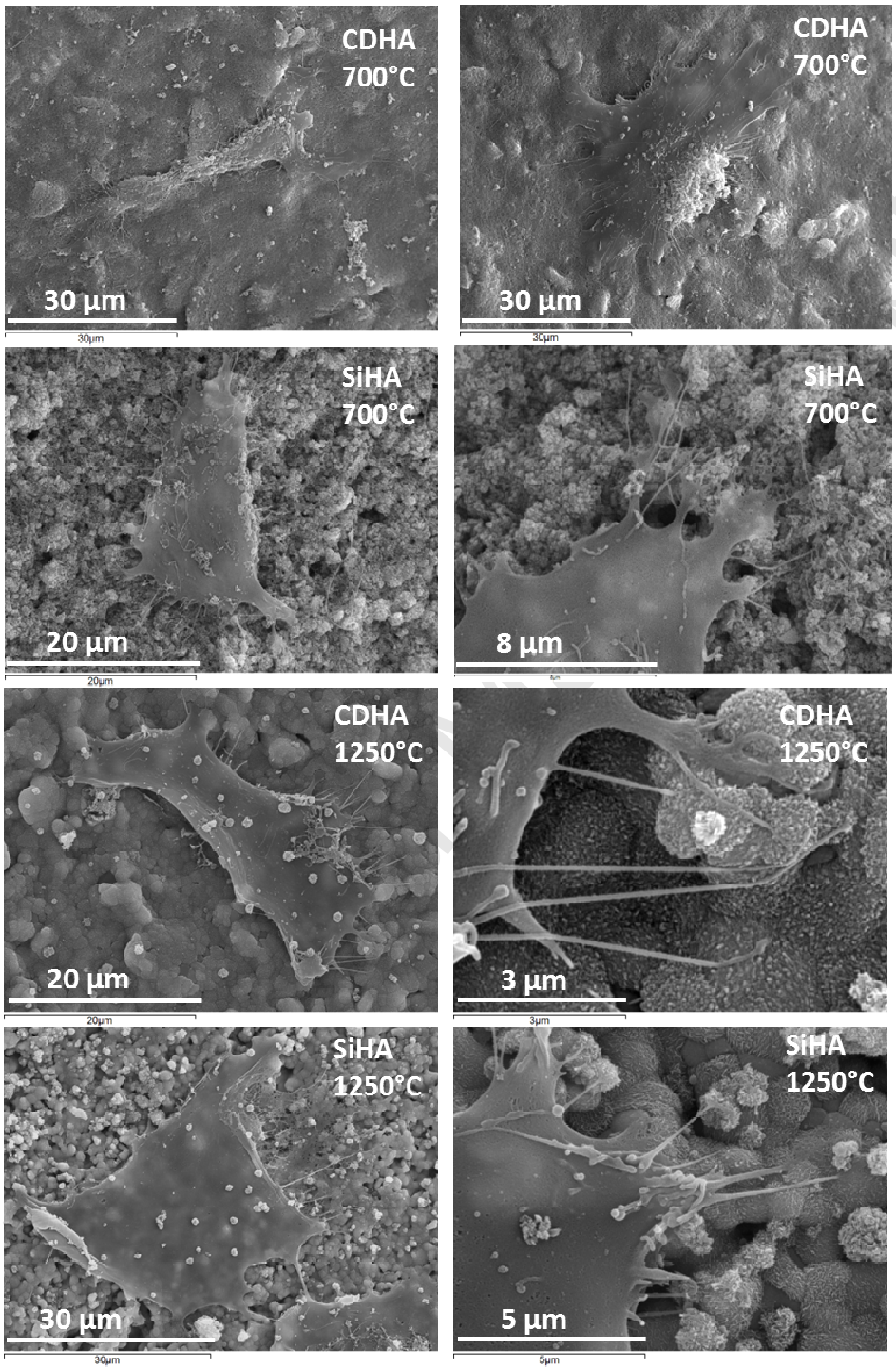

Figure 4. Morphology evaluation by SEM of Saos-2 osteoblast-like cells cultured for 48 hours on scaffolds of CDHA-700, SiHA-700, CDHA-1250 and SiHA-1250.

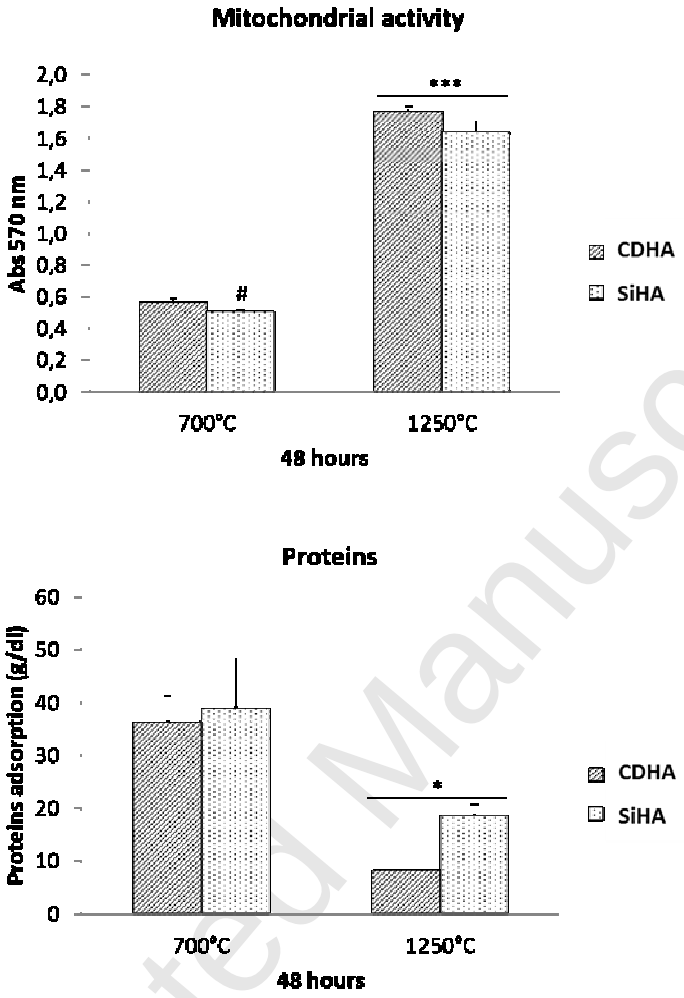

Figure 5. Mitochondrial activity and adsorption of medium proteins of Saos-2 osteoblast-like cells cultured for 48 hours on scaffolds of CDHA and SiHA treated at either 700ºC or 1250ºC. Data are expressed as means ± standard deviations (SD). All the experiments were performed twice and carried out in triplicate (n=6). Statistical significance: *$p<0.05$, ***$p<0.005$ (comparison between the same material at 700ºC and 1250ºC), #$p<0.05$ (comparison between CDHA and SiHA at the same temperature).

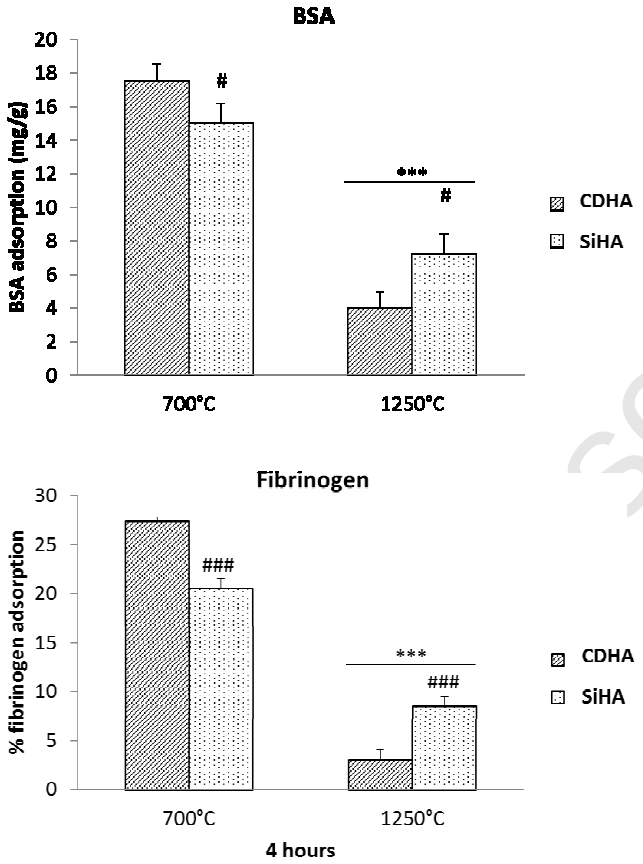

Figure 6. Adsorption of bovine serum albumin (BSA) and fibrinogen on powdered CDHA and SiHA. Data are expressed as means ± standard deviations (SD). All the experiments were performed twice and carried out in triplicate (n=6). Statistical significance: ***$p<0.005$ (comparison between the same material at 700ºC and 1250ºC), #$p<0.05$ and ###$p<0.005$ (comparison between CDHA and SiHA at the same temperature).

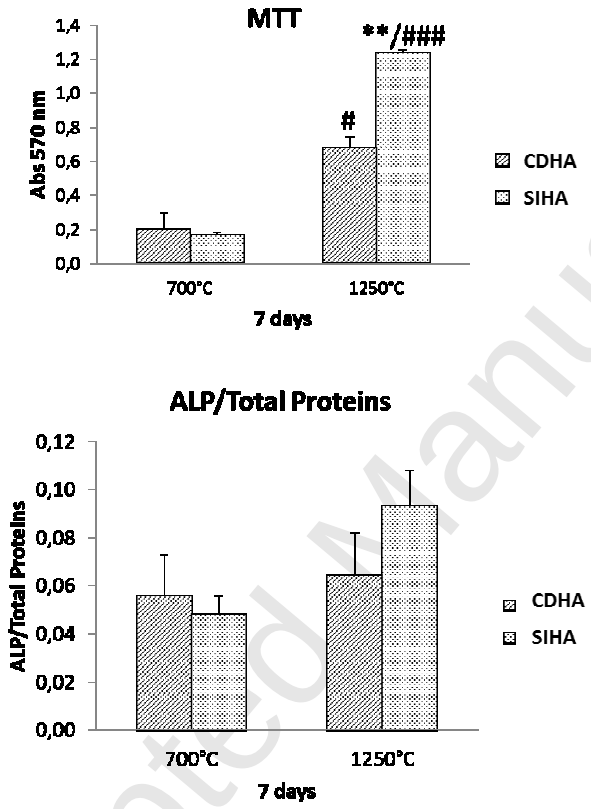

Figure 7. Mitochondrial activity and ALP activity of MC3T3 pre-osteoblast-like cells cultured for 7 days on scaffolds of CDHA and SiHA treated at either 700ºC or 1250ºC. Data are expressed as means ± standard deviations (SD). All the experiments were performed twice and carried out in triplicate (n=6). Statistical significance: **p<0.01 (comparison between CDHA and SiHA at the same temperature), #p<0.05 and ###p<0.005 (comparison between the same material at 700ºC and 1250ºC).

Table 1. Ca/P+Si ratio, phase composition, crystallite size, textural properties and ζ potential, for the scaffolds treated at 700º C and 1250º

Sample	Ca/P+Si ratio	Phase composition	Crystal Size (nm)	Surface area ($m^2 \cdot g^{-1}$)	Pore volume ($cm^3 \cdot g^{-1}$)	Pore size (nm)	ζ potential (mv)
CDHA-700	1.60	Apatite 100%	23.5	20.9	0.051	11.5	-19.5
SiHA-700	1.67	Apatite 100 %	33.4	36.6	0.105	11.5	-16.8
CDHA-1250	1.60	Apatite 61% α-TCP 39 %	77.5	0.2	-	-	-21.9
SiHA-1250	1.67	Apatite 85% α-TCP 15 %	63.6	1.1	-	-	-24.6

Acknowledgements

This study was supported by research grants from the Ministerio de Ciencia e Innovación (project MAT2012-35556), Ministerio de Economía y Competitividad (project MAT2013-43299-R) and Agening Network of Excellence (CSO2010-11384-E). M.C. Matesanz is greatly indebted to MEC for predoctoral fellowship. The authors wish to thank also to the staff of the ICTS Centro Nacional de Microscopia Electrónica (Spain) and Centro de Citometría y

Microscopia de Fluorescencia of the Universidad Complutense de Madrid (Spain) for the assistance in the scanning electron microscopy and flow cytometry studies, respectively.

Appendix A. Supplementary data

Additional information about FTIR spectroscopy carried out on powdered SiHA treated at 700ºC and 1250ºC, mechanical properties measured as a function of sintering temperature and cell culture texts of powdered samples.

References

[1] R.Z. Legeros, Chem. Rev. 108 (2008) 4742.

[2] J.H. Shepherd, S.M. Best, JOM 63 (2011) 83.

[3] D.W. Hutmacher, J.T. Schantz, C.X.F. Lam, K.C. Tan, T.C. Lim, J. Tissue Eng. Regen. Med. 1 (2007) 245.

[4] S.J. Hollister, Adv. Mater. 21 (2009) 3330.

[5] R. Langer, J.P. Vacanti, Science 260 (1993) 920.

[6] T.G. Kim, H. Sim, D.W. Lin, Adv. Funct. Mater. 22 (2012) 2446.

[7] M.J. Feito, R.M. Lozano, M. Alcaide, C. Ramírez-Santillán, D. Arcos, M. Vallet-Regí, M.T. Portolés, J. Mater. Sci. Mater. Med. 22 (2011) 405.

[8] D. Lozano, M.J. Feito, S. Portal-Nuñez, R.M. Lozano, M.C. Matesanz, M.C. Serrano, M. Vallet-Regí, M.T. Portolés, P. Esbrit, Acta Biomater. 8 (2012) 2770.

[9] F.M. Chen, M. Zhang, Z.F. Wu, Biomaterials 31 (2010) 6279.

[10] M. Mastrogiacomo, S. Scaglione, R. Martinetti, L. Dolcini, F. Beltrame, R. Cancedda, R. Quarto, Biomaterials 27 (2006) 3230.

[11] V. Karageorgiou, D. Kaplan, Biomaterials 26 (2005) 5474.

[12] P. Miranda, E. Saiz, K. Gryn, A.P. Tomsia, Acta Biomater. 2 (2006) 457.

[13] P. Miranda, A. Pajares, E. Saiz, A.P. Tomsia, F. Guiberteau, J. Biomed. Mater. Res. A 83 (2007) 646.

[14] F.J. Martínez-Vazquez, F.H. Perera, P. Miranda, A. Pajares, F. Guiberteau, Acta Biomater. 6 (2010) 4361.

[15] S.V. Dorozhkin, Biomaterials 31 (2010) 1465.

[16] M. Vallet-Regí, J. González-Calbet, Prog. Solid State Chem. 32 (2004) 1.

[17] P. Ducheyne, Q. Qiu, Biomaterials 20 (1999) 2287.

[18] M. Neo, T. Nakamura, T. Yamamuro, C. Ohtsuki, T. Kokubo, Reed Healthcare Communications (1993) 111.

[19] S.H. Maxian, J.P. Zawadski, M.G. Duna, J. Biomed. Mater. Res 27 (1993) 111.

[20] Y.R. Cai, Y.K. Liu, W.Q. Yan, Q.H. Hu, J.H. Tao, M. Zhang, Z.L. Shi, R.K. Tang, J. Mater. Chem. 17 (2007) 3780.

[21] W. van Raemdonck, P. Ducheyne, P. de Meester, in Metal and Ceramic Biomaterials, CRC Press, Boca Raton, 1984, p. 149.

[22] W. Suchanek, M. Yoshimura, J. Mater. Res. 13 (1998) 94.

[23] I.R. Gibson, S.M. Best, W. Bonfield, J. Biomed. Mater. Res. 44 (199) 422.

[24] D. Arcos, J. Rodriguez-Carvajal, M. Vallet-Regí, Chem. Mater. 16 (2004) 2300.

[25] M. Vallet-Regí, D. Arcos, J. Mater. Chem. 5 (2005) 1509.

[26] G. Daculsi, O. Laboux, O. Malard, P. Weiss, J. Mater. Sci. Mater. Med. 14 (2003) 195.

[27] S. Sánchez-Salcedo, I. Izquierdo-Barba, D. Arcos, M. Vallet-Regí, Tissue Eng. 12 (2006) 279.

[28] C.J. Wilson, R.E. Clegg, D.I. Leavesley, M.J. Pearcy, Tissue Eng. 11 (2005) 1.

[29] T. Mosmann, J. Immunol. Methods 65 (1983) 55.

[30] J. Reid, A. Pietak, M. Sayer, D. Dunfield, T.J.N. Smith, Biomaterials 26 (2005) 2887.

[31] M.C. Matesanz, M.J. Feito, C. Ramírez-Santillán, R.M. Lozano, S. Sánchez-Salcedo, D. Arcos, M. Vallet-Regí, M.T. Portolés, Macromol. Biosci. 12 (2012) 446.

[32] A. Quillet-Mary, J.P. Jaffrezou, V. Mansat, C. Bordier, J. Naval, G. Laurent, J. Biol. Chem. 272 (1997) 21388.

[33] F.M. Uckun, L. Tuclahlgren, C.W. Song, K. Waddick, D.E. Myers, J. Kirihara, J.A. Ledbetter. L. Schieven, Proc. Natl. Acad. Sci. USA 89 (1992) 9005.

[34] S. Burow, G. Valet, Eur. J. Cell. Biol. 43 (1987) 128.

[35] M. Alcaide, M.C. Serrano, J. Román, M.V. Cabañas, J. Peña, E. Sánchez-Zapardiel, M. Vallet-Regí, M.T. Portolés, J. Biomed. Mater. Res. A 95 (2010) 793.

[36] A. Nakajima, K. Yamada, L.B. Zou, Y. Yan, M. Mizuno, T. Nabeshima, Free Radic. Biol. Med. 32 (2002) 1324.

[37] A.J. Schmidt, J.-C. Krieg, H. Vedder, Prog. Neuro-Psychopharmacol. Biol. Psychiatry. 29 (2005) 321.

[38] E.S. Place, N.D. Evans, M. Stevens, Nature Mater. 8 (2009) 457.

[39] V. Demais, C. Audrain, G. Mabilleau, D. Chappard, M.F. Baslé, Morphologie 98 (2014) 53.

[40] Y. Lai, C. Xie, Z. Zhang, W. Lu, J. Ding, Biomaterials 31 (2010) 4809.

[41] M. Cicuéndez, M. Malmsten, J.C. Doadrio, M.T. Portolés, I. Izquierdo-Barba, M. Vallet-Regí, J. Mater. Chem. B 2 (2014) 49.

[42] M.B. Gorbet, M.V. Sefton, Biomaterials 25 (2004) 5681.

[43] A. Rosengren, E. Pavlovic, S. Oscarsson, A. Krajewski, A. Ravaglioli, A. Piancastelli, Biomaterials 23 (2002) 1237.

[44] Y. Wang, G. Subbiahdoss, J. de Vries, M. Libera, H.C. van der Mei, H.J. Busscher, Biofouling 28(2012) 1011.

[45] C. Tedjo, K.G. Neoh, E.T. Kang, N. Fang, V. Chan, J. Biomed. Mater. Res. A 82 (2007) 479.

[46] H. Chen, L. Yuan, W. Song, Z. Wu, D. Li, Prog. Polym. Sci. 33 (2008) 1059.

[47] B. Sivaraman, R.A. Latour, Biomaterials 31 (2010) 832.

[48] E. Mavropoulos, A.M. Costa, L.T. Costa, A.C. Achete, A. Mello, J.M. Granjeiro, A.M. Rossi, Colloid Surface B 83 (2011) 1.

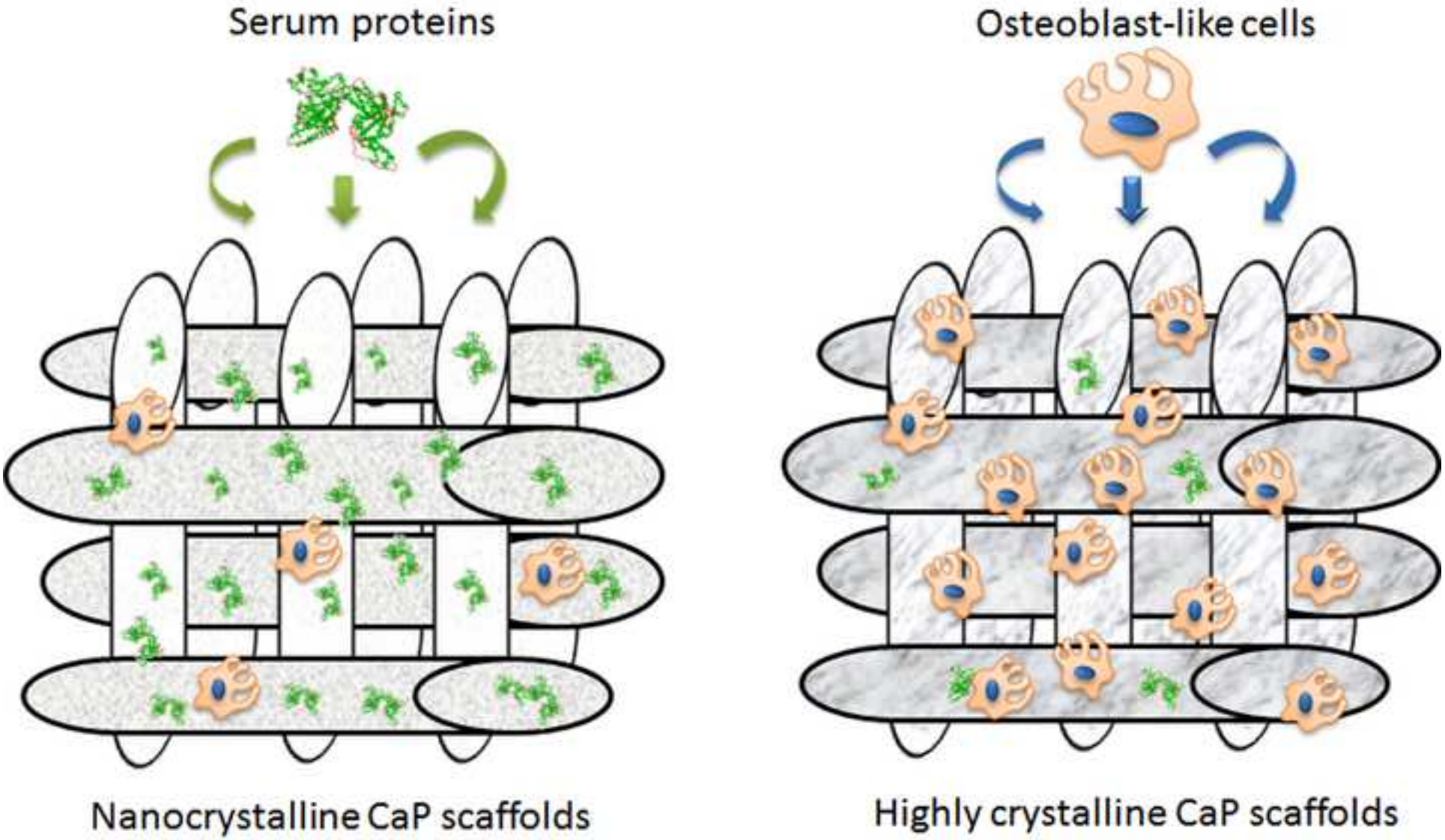
Serum proteins
Osteoblast-like cells
Nanocrystalline CaP scaffolds
Highly crystalline CaP scaffolds